

# The Synthetic Cannabinoid *R*(+)WIN 55,212-2 Inhibits the Interleukin-1 Signaling Pathway in Human Astrocytes in a Cannabinoid Receptor-independent Manner\*

Received for publication, July 21, 2005 Published, JBC Papers in Press, August 16, 2005, DOI 10.1074/jbc.M507959200

Niamh M. Curran, Bryan D. Griffin, Daniel O'Toole, Kevin J. Brady, Stephen N. Fitzgerald, and Paul N. Moynagh<sup>1</sup>

From the UCD School of Biomolecular and Biomedical Science, Conway Institute, University College Dublin, Belfield, Dublin 4, Ireland

*R*(+)WIN 55,212-2 is a synthetic cannabinoid that controls disease progression in models of multiple sclerosis. This is associated with its ability to reduce migration of leukocytes into the central nervous system. Because leukocyte migration is dependent on induction of adhesion molecules and chemokines by pro-inflammatory cytokines, we examined the effects of *R*(+)WIN 55,212-2 on their expression. Using 1321N1 astrocytoma and A-172 glioblastoma as cell models we show that *R*(+)WIN 55,212-2, but not its inactive chiral form *S*(-)WIN 55,212-2, strongly inhibits the interleukin-1 (IL-1) induction of the adhesion molecules intercellular adhesion molecule-1 (ICAM-1) and vascular cell adhesion molecule-1 (VCAM-1) and the chemokine IL-8. This inhibition is not mediated via the CB1 or CB2 cannabinoid receptors, because their selective antagonists and pertussis toxin failed to affect the inhibitory effects of *R*(+)WIN 55,212-2. Furthermore reverse transcription-PCR analysis did not detect the expression of either receptor in 1321N1 cells. *R*(+)WIN 55,212-2 was shown to inhibit adhesion molecule and chemokine expression at the level of transcription, because it strongly inhibited the IL-1 induction of ICAM-1, VCAM-1, and IL-8 mRNAs and blocked the IL-1 activation of their promoters. The NF $\kappa$ B pathway was then assessed as a lead target for *R*(+)WIN 55,212-2. NF $\kappa$ B was measured by expression of a transfected NF $\kappa$ B-regulated reporter gene. Using this assay, *R*(+)WIN 55,212-2 strongly inhibited IL-1 activation of NF $\kappa$ B. Furthermore *R*(+)WIN 55,212-2 inhibited the ability of overexpressed Myd88, Tak-1, and IKK-2 to induce the reporter gene suggesting that *R*(+)WIN 55,212-2 acts at or downstream of IKK-2 in the IL-1 pathway. However *R*(+)WIN 55,212-2 failed to inhibit IL-1-induced degradation of I $\kappa$ B $\alpha$ , excluding IKK-2 as a direct target. In addition electrophoretic mobility shift and chromatin immunoprecipitation assays showed that *R*(+)WIN 55,212-2 does not regulate the IL-1-induced nuclear translocation of NF $\kappa$ B or the ability of the latter to bind to promoters regulating expression of ICAM-1 and IL-8. These data suggest that *R*(+)WIN 55,212-2 blocks IL-1 signaling by inhibiting the transactivation potential of NF $\kappa$ B.

Inflammation in the CNS<sup>2</sup> is a key feature associated with neurodegenerative disorders, including multiple sclerosis (1). Reports have sug-

gested cannabinoids to be of potential therapeutic value in the treatment of such neuro-inflammatory conditions (2–4). More recently two concurrent reports demonstrated that the synthetic cannabinoid, *R*(+)WIN 55,212-2, ameliorates the progression of clinical disease in a murine model of multiple sclerosis (5, 6). These studies described anti-inflammatory activity of *R*(+)WIN 55,212-2 in the brain and its ability to inhibit leukocyte entry into the CNS. This is likely to be a key component underlying the therapeutic effects of *R*(+)WIN 55,212-2, because multiple sclerosis is an inflammatory-based disease characterized by a strong infiltration of the CNS by leukocytes (7). However, the molecular basis to the effects of *R*(+)WIN 55,212-2 was not addressed and the potential roles of the two G<sub>i</sub>-protein-coupled cannabinoid receptors (CB1 and CB2) (8) were not resolved. Because *R*(+)WIN 55,212-2 has been reported to inhibit the adhesion of leukocytes in the brain (9), we assessed the regulatory effects of *R*(+)WIN 55,212-2 on the expression of the likely adhesion molecules mediating this adhesion.

Adhesion molecules, such as VCAM-1 and ICAM-1, and chemokines, like IL-8, are elevated in multiple sclerosis lesions and make a major contribution to the extravasation of leukocytes across the blood-brain barrier (10–12). Indeed an antibody that blocks the interaction of leukocytes with VCAM-1 reduces the severity of experimental multiple sclerosis (13). The expression of adhesion molecules and chemokines in multiple sclerosis is prominent in astrocytes (11, 14). We and others have shown that the pro-inflammatory cytokine IL-1 is a key stimulus in the induction of VCAM-1, ICAM-1, and IL-8 in astrocytes (15–18). NF $\kappa$ B is a key driver in the induction processes, and IL-1 is a potent activator of this transcription factor in astrocytes (15, 19). The transcriptional activity of NF $\kappa$ B is tightly regulated by its association with the inhibitory I $\kappa$ B that sequesters NF $\kappa$ B in the cytosol. IL-1 causes phosphorylation of I $\kappa$ B proteins by the I $\kappa$ B-kinases (IKKs), IKK-1 and IKK-2, and this leads to I $\kappa$ B degradation. This allows for translocation of NF $\kappa$ B to the nucleus, where it activates genes encoding inflammatory proteins, including adhesion molecules. One of the most active subunits of NF $\kappa$ B is p65, and the transactivation potential of this subunit may be enhanced by phosphorylation at serine residues 276, 529, and 536 (20).

Our study demonstrates that *R*(+)WIN 55,212-2 inhibits the IL-1 induction of adhesion molecules, and IL-8 in astrocytes in a manner independent of CB1 and CB2 receptors. We also show that the likely mechanism is inhibition of the IL-1-induced transactivation of NF $\kappa$ B without affecting the degradation of I $\kappa$ B or the nuclear translocation or DNA binding of NF $\kappa$ B. This increases our molecular understanding of the anti-inflammatory effects of cannabinoids in the CNS.

\* This work was supported by Enterprise Ireland, the Health Research Board of Ireland, the Higher Education Authority of Ireland, and the European Commission. The costs of publication of this article were defrayed in part by the payment of page charges. This article must therefore be hereby marked "advertisement" in accordance with 18 U.S.C. Section 1734 solely to indicate this fact.

<sup>1</sup> To whom correspondence should be addressed. Tel.: 353-1-716-6761; Fax: 353-1-269-2749; E-mail: P.Moynagh@ucd.ie.

<sup>2</sup> The abbreviations used are: CNS, central nervous system; VCAM-1, vascular cell adhesion molecule-1; ICAM-1, intercellular adhesion molecule-1; IKKs, I $\kappa$ B-kinases; LDH, lactate dehydrogenase; IL-8, interleukin-8; PBS, phosphate-buffered saline; GAPDH,

glyceraldehyde-3-phosphate dehydrogenase; ChIP, chromosomal immunoprecipitation; RT, reverse transcription; MES, 4-morpholineethanesulfonic acid.

## R(+)*WIN 55,212-2* Inhibits Interleukin-1 Signaling

### EXPERIMENTAL PROCEDURES

**Materials**—The human 1321N1 astrocytoma was obtained from the European Collection of Animal Cell Cultures (Salisbury, UK). The human A-172 glioblastoma was from American Type Culture Collection (Manassas, VA). The Epstein-Barr virus-negative human B cell lymphoma BJAB cell line was a gift from Dr. D. Walls, Dublin City University, Ireland. Dulbecco's modified Eagle's medium, RPMI 1640, penicillin, streptomycin, fetal calf serum, and Superscript II reverse transcriptase were from Invitrogen. IL-1 $\beta$  was from NCI, National Institutes of Health (Frederick, MD). R(+)*WIN 55,212-2* and S(-)*WIN 55,212-2* were from Sigma-Aldrich. T4 polynucleotide kinase, the 22-bp oligonucleotide containing the NF $\kappa$ B consensus sequence (underlined) (5'-AGTTGAGGGGACTTTCACAGGC-3'), TaqDNA polymerase, dNTPs and the CytoTox 96 Non-Radioactive Cytotoxicity Assay were from Promega Corp. (Madison, WI). RNA ISOLATOR was from Genosys Biotechnologies, Inc. (Cambridge, UK). SR141716A and SR144528 were gifts from SANOFI-Recherche. Pertussis toxin was from Calbiochem-Novabiochem Ltd. Primers and probes for quantitative real-time PCR analysis of ICAM-1 (Hs00164932\_m1), VCAM-1 (Hs00174239\_m1), IL-8 (4309885P), and 18SrRNA (4310893E) were from Applied Biosystems (Foster City, CA). GeneJuice transfection reagent was from Novagen (Madison, WI). The NF $\kappa$ B-luciferase reporter plasmid ( $\kappa$ B-luc) consists of five copies of the NF $\kappa$ B consensus site cloned into the luciferase reporter construct pGL3-Basic (Promega Corp.). The ICAM-1-luciferase construct consists of 1344 bp of the ICAM-1 upstream region (-1353 to -9 relative to the start of transcription) cloned into the luciferase reporter vector pGL2 Basic and was a gift from Prof. Luke O'Neill (Trinity College Dublin, Ireland). The IL-8-luciferase reporter plasmid was a gift from Dr. Catherine Greene (Beaumont Hospital, Ireland). The construct encoding IKK-2 was from Tularik (San Francisco, CA). The construct encoding Tak-1 was a gift from H. Sakurai (Tanabe Seiyaku, Japan). The Luciferase Assay System with Reporter Lysis Buffer was from Promega Corp. (Madison, WI). [ $\gamma$ -<sup>32</sup>P]ATP was purchased from Amersham Biosciences. Rabbit polyclonal antibody against I $\kappa$ B- $\alpha$  and anti-p65 (sc-372) were obtained from Santa Cruz Biotechnology (Santa Cruz, CA). The antibody against phospho-Ser536 p65 and rabbit IgG was from Cell Signaling Technology (Milton Keynes, UK).

**Cell Culture**—1321N1 astrocytoma and A-172 glioblastoma were cultured in Dulbecco's modified Eagle's medium supplemented with 100 units/ml penicillin, 100  $\mu$ g/ml streptomycin, and 10% (v/v) fetal calf serum. The cells were passaged using 0.25% (w/v) trypsin in PBS. IL-1 $\beta$  stimulation was performed on cells in serum-containing medium at 37 °C for all experiments. Human BJAB cells were cultured in RPMI 1640 medium supplemented with 10% fetal calf serum, 2 mM L-glutamine, 100 units/ml penicillin, and 100  $\mu$ g/ml streptomycin. Cells were grown in a humidified atmosphere of 5% CO<sub>2</sub> at 37 °C.

**Enzyme-linked Immunosorbent Assay Detection of Cell Adhesion Molecules and IL-8**—1321N1 astrocytoma and A-172 glioblastoma (4  $\times$  10<sup>4</sup> cells/0.2 ml) were plated into 96-well microtiter plates and allowed to grow for 48 and 24 h, respectively. Cells were pre-treated for designated times with indicated concentrations of R(+)*WIN 55,212-2*, S(-)*WIN 55,212-2*, SR141716A, SR144528, or pertussis toxin prior to IL-1 $\beta$  (10 ng/ml) treatment for an additional 24 h. Stimulation was terminated by removal of medium, which was subsequently assayed for IL-8 using matched antibody pairs (R & D Systems Europe Ltd., Abingdon, Oxford, UK) in a sandwich enzyme-linked immunosorbent assay system according to the supplier's instruction. The adherent cells were measured for expression of VCAM-1 and ICAM-1 as described previously (15).

**Quantitative Real-time PCR Analysis of Adhesion Molecule and IL-8 Expression**—1321N1 astrocytoma (2  $\times$  10<sup>5</sup> cells/ml) were plated into 6-well plates and grown for 24 h. Cells were pre-treated for 1 h with R(+)*WIN 55,212-2* (20  $\mu$ M) prior to IL-1 $\beta$  (10 ng/ml) treatment for an additional 23 h. Cells were washed once with PBS, and RNA was extracted using Tri reagent (Sigma). After DNase I digestion, cDNA was generated from normalized RNA using SuperScript II reverse transcriptase. Samples were assayed by quantitative real-time PCR for levels of VCAM-1, ICAM-1, and IL-8 cDNA using the ABI Prism 7900HT thermal cycler. Reactions were performed using pre-validated primers and probes (Applied Biosystems).

**Assessment of Cytotoxicity Using the CytoTox 96 Non-radioactive Cytotoxicity Assay**—The effect of R(+)-*WIN 55,212-2* on 1321N1 cell viability was assessed by use of the CytoTox 96 non-radioactive cytotoxicity assay (Promega Corp.). This spectrophotometric method is based on the quantitative measurement of lactate dehydrogenase (LDH), a stable cytosolic enzyme that is released upon cell lysis, by a coupled enzymatic assay. 1321N1 astrocytoma (4  $\times$  10<sup>4</sup> cells/0.2 ml) were plated into 96-well microtiter plates and allowed to grow for 48 h. Cells were then treated with various concentrations of R(+)*WIN 55,212-2* as above. The cell medium was removed and assayed for LDH activity according to the manufacturer's instructions, and data were expressed relative to total LDH activity in the cells. The latter was measured in supernatants from untreated cells previously lysed in Triton X-100 (1% v/v).

**Assay of CB1 and CB2 mRNA Expression**—Total cellular RNA was prepared from 1321N1 astrocytoma and BJAB cells (4  $\times$  10<sup>6</sup> cells) using the RNA ISOLATOR according to the manufacturer's instructions. First strand cDNA synthesis was carried out using Superscript II reverse transcriptase and random oligonucleotide primers, and PCR amplification was performed using TaqDNA polymerase and primers to selectively amplify regions of the CB1, CB2, and GAPDH cDNAs. The sequences of the forward and reverse oligonucleotide primers and the sizes of the products were: CB1, 5'-GAGACAACCCCCAGCTAGTCCAGCAGACC-3' and 5'-TGGGCCTGGTGACAATCCTCTTAT-AGGCC-3', 500 bp; CB2, 5'-CTTCTGGCCCTGCTAAGTGCCCTG-GAGAACG-3' and 5'-CAGCAAGTCCATCCCATGAGGGGCAGC-TAGG-3', 400 bp; and GAPDH, 5'-ACCACAGTCCATGCCATC-3' and 5'-TCCACCACCCTGTTGCTG-3', 452 bp. Amplification parameters were as follows: step 1: 35 cycles at 94 °C for 1 min, at 53 °C for 1 min and at 72 °C for 1 min; step 2: at 72 °C for 10 min. The PCR products were subjected to electrophoresis on a 1.5% agarose gel, containing ethidium bromide, and photographed.

**Cell Transfections**—1321N1 astrocytoma (4  $\times$  10<sup>4</sup> cells/0.2 ml) were plated into 96-well microtiter plates and allowed to grow for 24 h. Cells were then transfected, using GeneJuice transfection reagent, with designated firefly luciferase reporter plasmids (80–100 ng), constitutively expressed *Renilla*-luciferase reporter construct (phRL-TK) (40 ng), and expression constructs encoding Myd88, Tak-1, or IKK-2 (80 ng). In control experiments lacking the latter expression constructs total DNA was kept constant (240 ng/well) using the pcDNA3.1 empty vector. Cells were allowed to recover overnight (17 h) and then pre-treated with or without R(+)*WIN 55,212-2* or S(-)*WIN 55,212-2* for 1 h prior to stimulation in the presence or absence of IL-1 (10 ng/ml) for a further 6 h. Cell extracts were generated using the Reporter lysis buffer (Promega), and extracts were assayed for firefly luciferase and *Renilla*-luciferase activity using the Luciferase assay system (Promega) and coelenterazine (1  $\mu$ g/ml), respectively.

**Preparation of Nuclear and Cytosolic Fractions**—1321N1 cells (2  $\times$  10<sup>5</sup> cells/ml; 3 ml) were seeded into 6-well plates and allowed to adhere

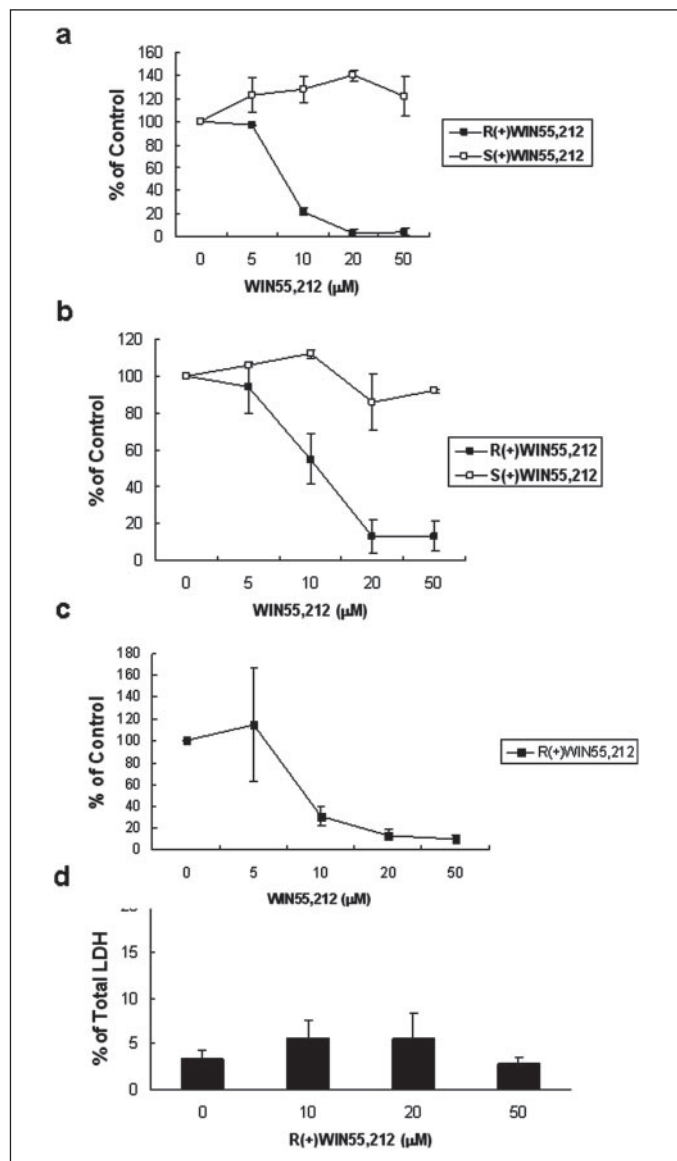


**FIGURE 1. R(+)-WIN 55,212-2 inhibits IL-1 $\beta$ -induction of ICAM-1, VCAM-1, and IL-8 in 1321N1 astrocytoma.** 1321N1 astrocytoma were pretreated for 1 h with various concentrations of the *R* and *S* enantiomers of WIN 55,212-2 and stimulated for a further 24-h period with IL-1 $\beta$  (10 ng/ml). The cells were then measured for ICAM-1 (a), VCAM-1 (b), and IL-8 (c) expression by direct and sandwich enzyme-linked immunosorbent assay as described under "Experimental Procedures." The results are expressed as percentages of values obtained in IL-1 $\beta$ -treated cells in the absence of WIN 55,212-2. d, 1321N1 astrocytoma were treated with various concentrations of *R*(+)-WIN 55,212-2 for 24 h and then assessed for viability by measuring LDH release in the conditioned medium as described under "Experimental Procedures." The LDH release is expressed as percentage of total LDH in the cells. The data represent mean  $\pm$  S.E. of three independent experiments.

for 72 h. Cells were pre-treated with or without various concentrations of *R*(+)-WIN 55,212-2 or *S*(-)-WIN 55,212-2 for 1 h prior to stimulation in the presence or absence of IL-1 (10 ng/ml) for 30 min. Stimulation was terminated by removal of medium, and cells were washed with 5 ml of ice-cold PBS. Cells were then scraped into 1 ml of ice-cold hypotonic buffer (10 mM HEPES-NaOH buffer, pH 7.9, containing 1.5 mM MgCl<sub>2</sub>, 10 mM KCl, 0.5 mM dithiothreitol, and 0.5 mM phenylmethylsulfonyl fluoride). Cells were pelleted by centrifugation at 14,000  $\times$  *g* for 10 min and then lysed for 10 min on ice in hypotonic buffer (20  $\mu$ l) containing 0.1% (v/v) Nonidet P-40. Lysates were centrifuged at 14,000  $\times$  *g* for 10 min. The resulting supernatants constituted cytosolic fractions and were measured for levels of I $\kappa$ B by Western immunoblotting as

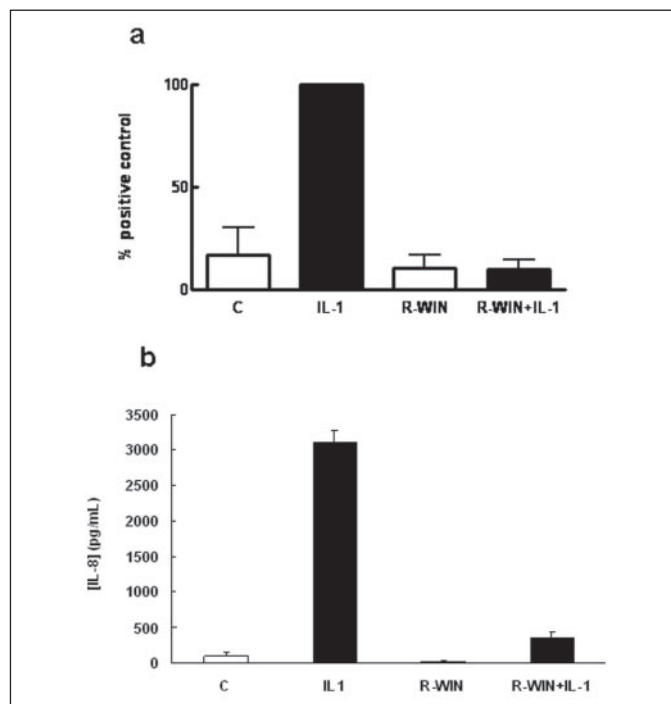


**FIGURE 2. R(+)-WIN 55,212-2 inhibits IL-1 $\beta$  induction of ICAM-1 and IL-8 in A-172 glioblastoma.** A-172 glioblastoma were pretreated for 1 h with *R*(+)-WIN 55,212-2 (20  $\mu$ M) and stimulated for a further 24-h period with IL-1 $\beta$  (10 ng/ml). The cells were then measured for ICAM-1 (a) and IL-8 (b) expression by direct and sandwich enzyme-linked immunosorbent assay respectively as described under "Experimental Procedures." The ICAM data are expressed as percentages of values obtained in IL-1 $\beta$ -treated cells in the absence of WIN 55,212-2. The data represent mean  $\pm$  S.E. of three independent experiments.

described previously (19). The pellets were resuspended in 20 mM HEPES-NaOH buffer, pH 7.9 (15  $\mu$ l), containing 420 mM NaCl, 1.5 mM MgCl<sub>2</sub>, 0.2 mM EDTA, 25% (w/v) glycerol, and 0.5 mM phenylmethylsulfonyl fluoride and incubated for 15 min on ice. Incubations were then centrifuged at 14,000  $\times$  *g* for 10 min, and the supernatants were removed into 10 mM HEPES-NaOH buffer, pH 7.9 (75  $\mu$ l), containing 50 mM KCl, 0.2 mM EDTA, 20% (w/v) glycerol, 0.5 mM phenylmethylsulfonyl fluoride, and 0.5 mM dithiothreitol. Such samples constituted nuclear extracts and were assayed for NF $\kappa$ B by the electrophoretic mobility shift assay.

**Electrophoretic Mobility Shift Assay**—Nuclear extracts (10  $\mu$ g of protein) were incubated with 30,000 dpm of a 22-bp oligonucleotide containing the NF $\kappa$ B consensus sequence, which previously had been labeled with [ $\gamma$ -<sup>32</sup>P]ATP (10 mCi/mmol) by T4 polynucleotide kinase (19). Incubations were performed for 30 min at room temperature in 10 mM Tris-HCl buffer, pH 7.5, containing 100 mM NaCl, 1 mM EDTA, 5 mM dithiothreitol, 4% (w/v) glycerol, 2  $\mu$ g of poly(dI-dC), and 1 mg/ml nuclease-free bovine serum albumin. All incubations were subjected to electrophoresis on native 4% (w/v) polyacrylamide gels that were subsequently dried and autoradiographed.

**Chromatin Immunoprecipitation and Analysis by Quantitative Real-time PCR**—1321N1 astrocytoma cells were grown to confluency in 90-mm dishes. Cells were pre-treated with or without *R*(+)-WIN 55,212-2 (20  $\mu$ M) for 1 h prior to stimulation in the absence or presence of IL-1 $\beta$  (10 ng/ml) for 1 h. ChIP assays were performed as previously described (21) with some modifications. Following stimulation, cells were cross-linked with 1% (v/v) formaldehyde for 10 min at 37  $^{\circ}$ C. Isolated nuclei were subjected to seven 10-s sonication pulses from a Sanyo/MES Soniprep 150 at one-third of total power. Separate aliquots from each chromatin preparation were incubated overnight at 4  $^{\circ}$ C with

**FIGURE 3. R(+)-WIN 55,212-2 inhibits IL-1 induction of adhesion molecules in a cannabinoid receptor independent manner.** 1321N1 astrocytoma were challenged for 1 h with SR141716A (10  $\mu$ M) (a and b) or SR144528 (10  $\mu$ M) (c and d) prior to treatment with or without R(+)-WIN 55,212-2 (20  $\mu$ M) for 1 h and further stimulation for 24 h with IL-1 $\beta$  (10 ng/ml). The cells were then measured for ICAM-1 (a and c) and VCAM-1 (b and d) expression, and results are expressed as percentages of values obtained in IL-1 $\beta$ -treated cells in the absence of R(+)-WIN 55,212-2. The data represent mean  $\pm$  S.E. of three independent experiments.

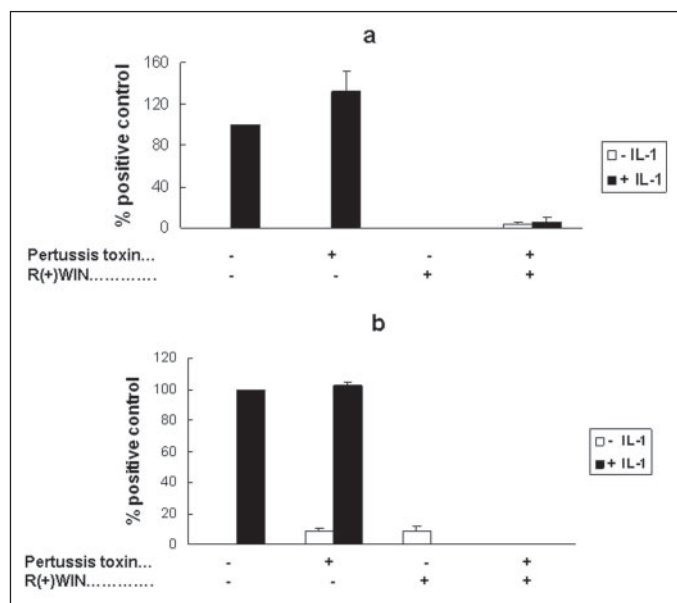
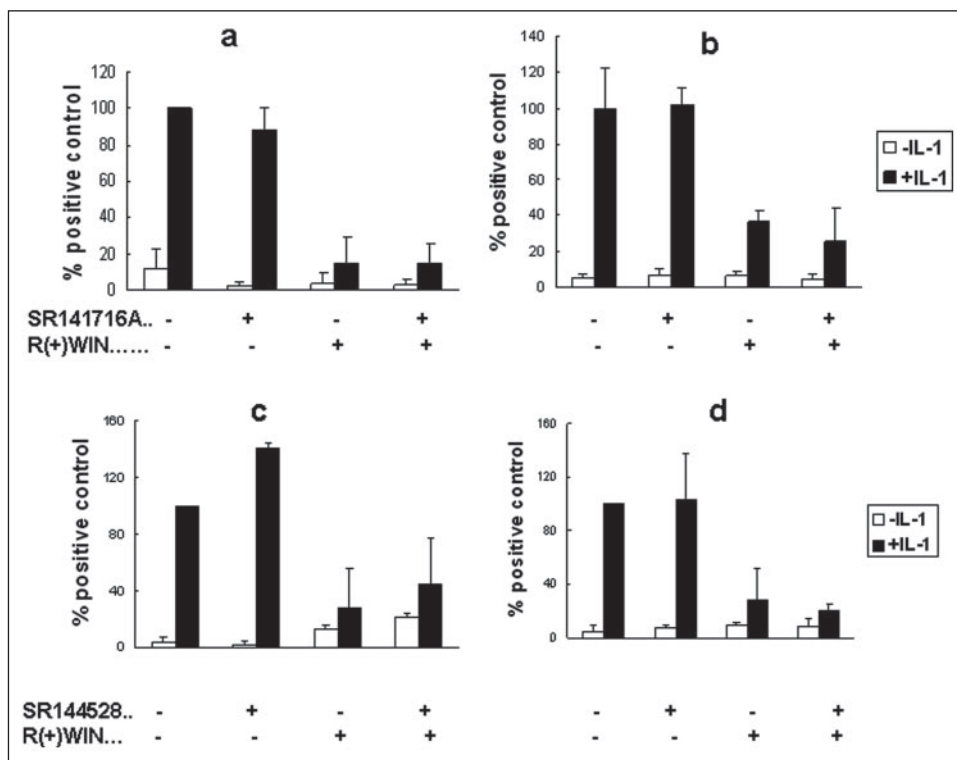


**FIGURE 4. R(+)-WIN 55,212-2 inhibits IL-1 induction of adhesion molecules independently of G $\beta$  protein.** 1321N1 astrocytoma were challenged overnight with pertussis toxin (50 ng/ml) prior to treatment with or without R(+)-WIN 55,212-2 (20  $\mu$ M) for 1 h and further stimulation for 24 h with IL-1 $\beta$  (10 ng/ml). The cells were then measured for ICAM-1 (a) and VCAM-1 (b) expression, and results are expressed as percentages of values obtained in IL-1 $\beta$ -treated cells in the absence of R(+)-WIN 55,212-2. The data represent mean  $\pm$  S.E. of three independent experiments.

anti-p65 antibody and rabbit IgG antibody. An aliquot was also retained as an input sample to normalize PCR reactions and analyze shearing efficiency. Chromatin used had an average size of 750 bp. After reversal of cross-links by overnight incubation at 65  $^{\circ}$ C, DNA was extracted using the QIAquick purification kit (Qiagen) according to the manufacturer's instructions. Standard PCR was performed using 1  $\mu$ l (~3% of total) of template DNA, 500 nM primers, and 0.2 unit of TaqDNA polymerase (Invitrogen) per 50- $\mu$ l reaction. Quantitative real-time PCR

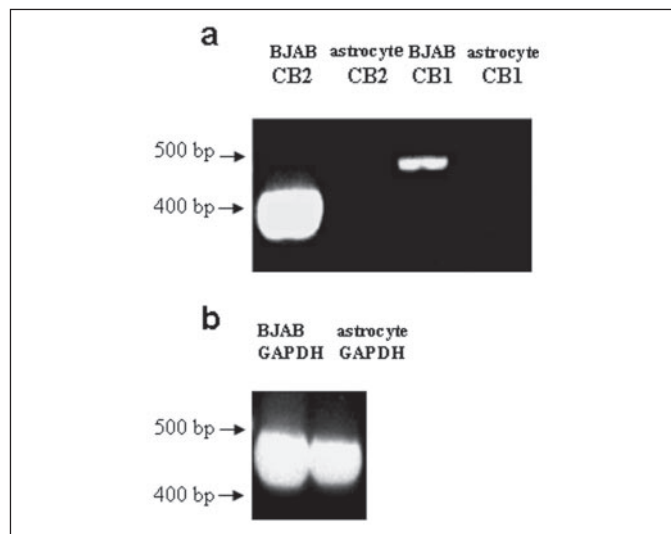


**FIGURE 5. Lack of expression of CB1 and CB2 receptors in 1321N1 astrocytoma.** Total cellular RNA was prepared from BJAB and 1321N1 astrocyte cells and subjected to first strand cDNA synthesis using Superscript II reverse transcriptase and random oligonucleotide primers. PCR amplification was performed using TaqDNA polymerase and primers to selectively amplify regions of CB1 (a) and CB2 and GAPDH (b) cDNAs. This resulted in the generation of products with the predicted sizes of 500 bp, 400 bp, and 452 bp, respectively.

reactions were performed in duplicate with 2  $\mu$ l of template DNA, 50 nM primers, and the SYBR Green Jumpstart Taq Readymix (Sigma), using the Mx3000P QPCR System (Stratagene). Dissociation curve analysis and gel electrophoresis of the final products confirmed that only the expected specific amplicon of correct size was generated for each target promoter. Real-time PCR data analysis was performed as previously described (22). Results for each treatment are expressed as -fold differences between DNA enrichment in the p65-ChIP sample relative to IgG-ChIP sample. The sequences of primers used are as follows: ICAM-1, 5'-CTCCACTCTCCGGGGAAGTTG-3' and 5'-GCTG-

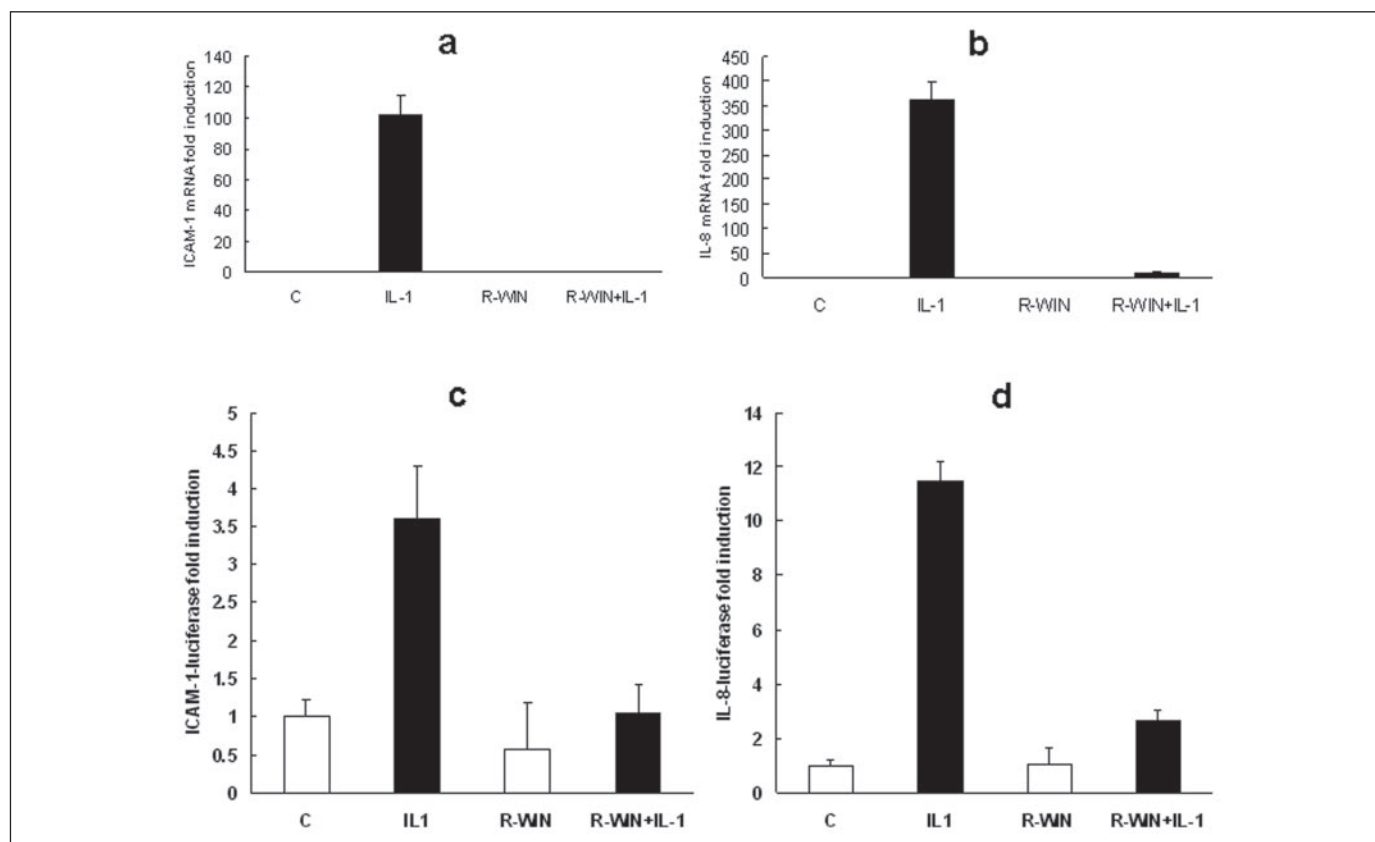


FIGURE 6. R(+)-WIN 55,212-2 inhibits IL-1 induction of mRNAs encoding ICAM-1 and IL-8 and IL-1 activation of ICAM-1 and IL-8 promoters. *a* and *b*, 1321N1 astrocytoma were pre-treated for 1 h with R(+)-WIN 55,212-2 (20  $\mu$ M) prior to IL-1 $\beta$  (10 ng/ml) treatment for an additional 23 h. RNA extracts were generated and converted into cDNA. Samples were assayed by quantitative real-time PCR for levels of ICAM-1 (*a*) and IL-8 (*b*) mRNA using the ABI Prism 7900HT thermal cycler. *c* and *d*, 1321N1 cells were co-transfected with ICAM-1 promoter luciferase (100 ng, *c*), IL-8 promoter luciferase (100 ng, *d*), pRL-TK (constitutively expressed *Renilla* luciferase) (40 ng) and pcDNA3.1 (80 ng). Cells were allowed to recover overnight and then pre-treated with or without R(+)-WIN 55,212-2 (20  $\mu$ M) for 1 h prior to stimulation in the presence or absence of IL-1 (10 ng/ml) for a further 6 h. Data are expressed relative to levels in control unstimulated cells (*c*) and represent mean  $\pm$  S.E. of two experiments.

CAGTTATTTCCGGACTGAC-3'; IL-8, 5'-GGAAGTGTGATGAC-TCAGGTTTGC-3' and 5'-GATGGTTCCTCCGGTGGTTTCT-TC-3'; and GAPDH, 5'-CTACTAGCGGTTTACGGGCG-3' and 5'-TCGAACAGGAGGAGCAGAGAGCGA-3'.

**Western Blot Analysis of p65 Phosphorylation**—1321N1 astrocytoma ( $2 \times 10^5$  cells/ml; 3 ml) were plated into 6-well plates and allowed to grow for 24 h. Cells were pre-treated with or without R(+)-WIN 55,212-2 for 1 h prior to stimulation in the presence or absence of IL-1 (10 ng/ml) for 30 min. Stimulation was terminated by removal of medium, and the adherent cells washed with ice-cold PBS (3 ml). The cells were then scraped into PBS (1 ml) and pelleted by centrifugation at  $21,000 \times g$  for 5 min at 4  $^{\circ}$ C. The cell pellets were lysed in SDS-PAGE sample buffer (100  $\mu$ l, 50 mM Tris-HCl buffer, pH 6.8, containing 2% (w/v) SDS, 10% glycerol, 1% (v/v) 2-mercaptoethanol, and 0.1% bromophenol blue). The lysates were sonicated for 10 s to reduce sample viscosity and then heated to 90  $^{\circ}$ C for 5 min. Lysates (20  $\mu$ l) were subjected to SDS-PAGE on 10% polyacrylamide slab gels, and the separated proteins were electrophoretically transferred from the gels to nitrocellulose. The nitrocellulose was then probed for levels of Ser536 phosphorylated using specific antibodies as recommended by the manufacturers. Immunoreactivity was visualized by enhanced chemiluminescence.

## RESULTS

Because R(+)-WIN 55,212-2 has been reported to inhibit the infiltration of leukocytes into the brain (9), we initially assessed the regulatory effects of R(+)-WIN 55,212-2 on the expression of the likely adhesion molecules and chemokines mediating this infiltration process. We have

previously characterized the ability of IL-1 to induce the expression of the adhesion molecules VCAM-1 and ICAM-1 and the chemokine IL-8 in human 1321N1 astrocytoma cells (15, 18), and this was used as the model in the present study. R(+)-WIN 55,212-2 was assessed for its ability to inhibit the IL-1 induction of adhesion molecules and IL-8 in this cell system (Fig. 1). R(+)-WIN 55,212-2 caused a dose-dependent inhibition of the IL-1 induction of both ICAM-1 (Fig. 1*a*), VCAM-1 (Fig. 1*b*), and IL-8 (Fig. 1*c*) in 1321N1 astrocytoma. The dose-dependent inhibitory profiles were similar in all three cases. WIN 55,212-2 is available in two enantiomeric forms, *R* and *S*, with *R* being the active form (23). In contrast to the *R* form, the inactive chiral *S*(-)-WIN 55,212-2 failed to affect the ability of IL-1 to induce ICAM-1 (Fig. 1*a*) and VCAM-1 (Fig. 1*b*) suggesting that a stereoselective mechanism underlies the inhibitory effects of R(+)-WIN 55,212-2. To exclude the possibility that the inhibitory effects of R(+)-WIN 55,212-2 were due indirectly to nonspecific cytotoxicity, the viability of the cells after treatment with the same concentration range of R(+)-WIN 55,212-2 was assessed by measuring the release of LDH (Fig. 1*d*). None of the concentrations of R(+)-WIN 55,212-2 caused any detrimental effects on cellular viability indicating that its inhibitory effects on VCAM-1 and ICAM-1 expression are not due to general toxicity.

To ensure that the above effects are not simply artifacts of the 1321N1 astrocytoma cell line, the effect of R(+)-WIN 55,212-2 on A-172 glioblastoma, another cell of glia origin, was next examined. Like 1321N1 astrocytoma, A-172 cells showed increased expression of adhesion molecules such as ICAM-1 (Fig. 2*a*) and the chemokine IL-8 (Fig. 2*b*) in response to IL-1. The pre-treatment of A-172 cells with R(+)-WIN

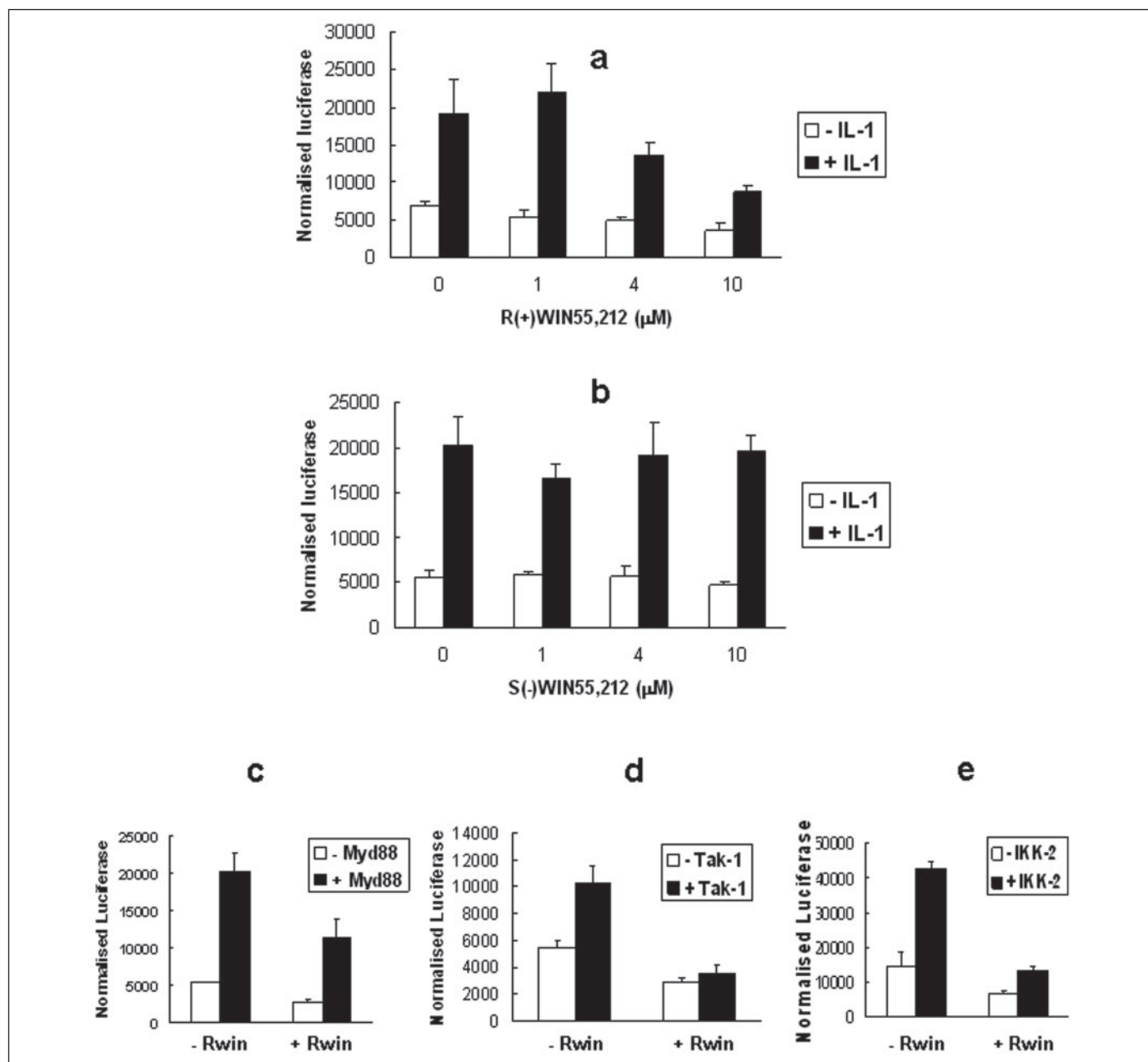


FIGURE 7. *R(+)*WIN 55,212-2 inhibits IL-1 induction of NFκB-regulated reporter gene in 1321N1 astrocytoma. *a* and *b*, 1321N1 cells were co-transfected with a NFκB-regulated firefly luciferase reporter (80 ng), phRL-TK (constitutively expressed *Renilla* luciferase) (80 ng), and pcDNA3.1 (80 ng). Cells were allowed to recover overnight and then pre-treated with or without various concentrations of *R(+)*WIN 55,212-2 (*a*) or *S(-)*WIN 55,212-2 (*b*) for 1 h prior to stimulation in the presence or absence of IL-1 (10 ng/ml) for a further 6 h. *c-e*, 1321N1 cells were co-transfected with a NFκB-regulated firefly luciferase reporter (80 ng), phRL-TK (constitutively expressed *Renilla* luciferase) (80 ng), and pcDNA3.1 (80 ng) or expression plasmids encoding Myd88 (*c*), Tak-1 (*d*), or IKK-2 (*e*) (80 ng). Cells were allowed to recover overnight and then treated with or without *R(+)*WIN 55,212-2 (20 μM) for 7 h. Cell extracts were generated and assayed for firefly and *Renilla* (for normalizing transfection efficiency) luciferase. Data are presented as normalized firefly luciferase activity.

55,212-2 caused a complete blockade of the IL-1 induction of ICAM-1 (Fig. 2*a*) and IL-8 (Fig. 2*b*) thus validating the previous findings from 1321N1 astrocytoma.

The involvement of the cannabinoid receptors CB1 and CB2 in mediating the inhibitory effects of *R(+)*WIN 55,212-2 was next explored by assessing the ability of the CB1 and CB2 receptor antagonists, SR141716A and SR144528, respectively, to regulate the inhibitory effects of *R(+)*WIN 55,212-2 in 1321N1 cells. SR141716A had no influence on the IL-1 induction of ICAM-1 but more importantly failed to affect the strong inhibitory effects of *R(+)*WIN 55,212-2 on the induction process (Fig. 3*a*). Similar results were obtained with respect to VCAM-1 expression (Fig. 3*b*). This indicates a lack of involvement of

the CB1 receptor in mediating the inhibitory effects. The role of the CB2 receptor was next examined by assessing the regulatory effects of SR144528 on *R(+)*WIN 55,212-2. However, like the CB1 receptor antagonist, SR144528 failed to regulate the strong inhibitory effects of *R(+)*WIN 55,212-2 on IL-1 induction of ICAM-1 (Fig. 3*c*) or VCAM-1 (Fig. 3*d*) in 1321N1 cells and thus tended to exclude a role for the CB2 receptor in mediating the effects of *R(+)*WIN 55,212-2.

Because both CB1 and CB2 receptors signal via a G<sub>i</sub> protein, and the latter is subject to inhibition by pertussis toxin, the roles of CB1 and CB2 receptors were further probed by investigating the regulation of the effects of *R(+)*WIN 55,212-2 by this toxin. However the inability of pertussis toxin to modulate the inhibitory effects of *R(+)*WIN 55,212-2

on IL-1 induction of ICAM-1 (Fig. 4a) or VCAM-1 (Fig. 4b) further confirms the lack of involvement of the CB1 and CB2 receptors in mediating the responses to *R(+)*WIN 55,212-2.

The above findings prompted an analysis of the expression levels of the two receptors in 1321N1 astrocytoma. The highly sensitive approach of RT-PCR was exploited to amplify the CB1 and CB2 receptors by using primers that specifically amplify regions of the CB1 or CB2 receptor cDNAs. The BJAB cell line was also probed for expression of both receptor subtypes and acted as a positive control for the primers and RT-PCR procedure, since it has previously been shown that B cells express high levels of cannabinoid receptors (24). Indeed the RT-PCR analysis in the present study resulted in the generation of products with the predicted sizes of 500 bp (CB1) and 400 bp (CB2) in BJAB cells (Fig. 5a) demonstrating that these cells express both CB1 and CB2. In addition the generation of these products validates the primers and PCR conditions as a suitable detection system for the expression of both receptors. Intriguingly, the equivalent RT-PCR analysis of RNA from 1321N1 astrocytoma failed to generate any such products indicating that these cells do not express the CB1 and CB2 receptors (Fig. 5a). To confirm the RNA from 1321N1 cells as a suitable source for RT-PCR analysis, primers were also used to amplify a region of the housekeeping GAPDH gene (Fig. 5b). This resulted in the generation of a PCR product of the predicted 452-bp size with BJAB and 1321N1 cells both displaying comparable levels of the product. This indicates the absence of expression of CB1 and CB2 receptors in 1321N1 astrocytoma and unambiguously confirms that the inhibitory effects of *R(+)*WIN 55,212-2 on adhesion molecule and chemokines expression in glial cells are mediated by a mechanism independent of these receptors.

In an effort to delineate the mechanism underlying the inhibitory effects of *R(+)*WIN 55,212-2, transcriptional regulation of adhesion molecule and chemokine expression by IL-1 was probed as a potential target for *R(+)*WIN 55,212-2. Real-time PCR was used to quantitate levels of mRNA encoding ICAM-1, VCAM-1, and IL-8. IL-1 caused over 100-fold induction of ICAM-1 mRNA in 1321N1 cells, and this was blocked by pre-treatment with *R(+)*WIN 55,212-2 (Fig. 6a). Similarly IL-1 caused robust induction of IL-8 mRNA in these cells, and again this was inhibited by *R(+)*WIN 55,212-2 (Fig. 6b). IL-1 also strongly induced VCAM-1 mRNA in 1321N1 cells, but because this mRNA species was undetectable in untreated cells it was not possible to express -fold induction by IL-1. It is worth noting, however, that *R(+)*WIN 55,212-2 inhibited, by 80%, the induction of VCAM-1 by IL-1 (data not shown). To further characterize the inhibitory effects of *R(+)*WIN 55,212-2 on the transcription of ICAM-1 and IL-8, its effects on the IL-1 activation of luciferase that is regulated by the ICAM-1 promoter, and this was blocked by *R(+)*WIN 55,212-2 (Fig. 6c). IL-1 caused even stronger induction of luciferase that is regulated by the IL-8 promoter, and again this was inhibited by *R(+)*WIN 55,212-2 (Fig. 6d).

The inhibitory effects of *R(+)*WIN 55,212-2 on the IL-1 activation of the ICAM-1 and IL-8 promoters and the ensuing blockade of IL-1 induced transcription of ICAM-1 and IL-8 suggested that transcription factors regulating these promoters may be key targets for *R(+)*WIN 55,212-2. The crucial role of NFκB in IL-1 signaling coupled to its regulation of adhesion molecule and chemokine expression in astrocytes (15, 18) promoted it as a lead candidate. *R(+)*WIN 55,212-2 was initially examined for its effects on IL-1 induction of a NFκB-regulated reporter gene. *R(+)*WIN 55,212-2 caused a strong and dose-dependent inhibition of the IL-1 induction of the reporter gene (Fig. 7a), whereas its chiral form *S(-)*WIN 55,212-2 was ineffective (Fig. 7b). In an effort to further resolve the point of the IL-1 pathway that is subject to inhibition

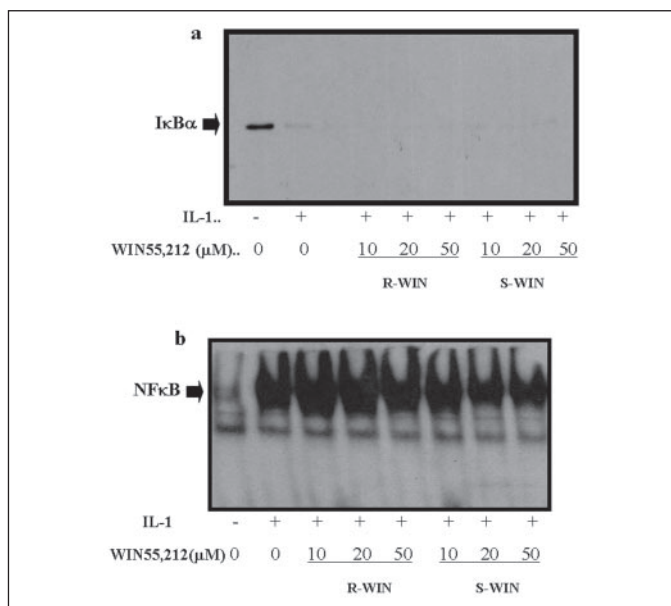


FIGURE 8. *R(+)*WIN 55,212-2 does not regulate IL-1-induced degradation of IκB, nuclear translocation, or DNA binding of NFκB. 1321N1 astrocytoma were pretreated for 1 h with various concentrations of the *R* and *S* enantiomers of WIN 55,212-2 and stimulated for a further 30 min with IL-1β (10 ng/ml). *a*, cytosolic extracts were prepared and analyzed by Western immunoblotting for levels of IκBα. *b*, nuclear extracts were prepared and assessed for NFκB activity by electrophoretic mobility shift assay.

by *R(+)*WIN 55,212-2, the sensitivity of a number of signaling molecules at various stages in the IL-1 pathway was examined. Thus Myd88, Tak-1, and IKK-2 were overexpressed and shown to cause robust induction of the NFκB-regulated reporter gene (Fig. 7, *c–e*). Interestingly *R(+)*WIN 55,212-2 strongly inhibited the ability of each of the signaling molecules to induce the reporter gene suggesting that it targets the IL-1 pathway at or downstream of IKK-2.

Because IKK-2 directly phosphorylates the IκB proteins leading to their degradation, IKK-2 was assessed as a target by probing the effects of *R(+)*WIN 55,212-2 on IL-1-induced degradation of IκBα. IL-1 caused complete degradation of IκBα after 30 min, but neither *R(+)*WIN 55,212-2 nor its chiral *S* form inhibited this degradation indicating that the IKKs are not direct targets for *R(+)*WIN 55,212-2 (Fig. 8a).

The degradation of IκB is followed by nuclear translocation of NFκB and its subsequent binding to DNA motifs in specific promoters. Thus these steps were also examined as potential targets for *R(+)*WIN 55,212-2. This was initially performed by generating nuclear extracts and measuring for binding to oligonucleotides containing the consensus NFκB motif by the electrophoretic mobility shift assay. IL-1 caused the strong activation of NFκB in this assay as judged by the increased intensity of the retarded NFκB-DNA complexes in IL-1-treated cells (Fig. 8b). Pre-treatment with either form of WIN 55,212-2 failed to affect this activation suggesting that *R(+)*WIN 55,212-2 does not target the nuclear translocation or DNA-binding capacity of NFκB.

More specific studies were performed to characterize the effects of *R(+)*WIN 55,212-2 on the specific binding of NFκB to the ICAM-1 and IL-8 promoters. Because the *in vivo* binding of transcription factors to DNA occurs within the context of intact chromatin structures, CHIP assays were performed to evaluate whether *R(+)*WIN 55,212-2 could affect the binding of the NFκB subunit, p65, to the ICAM-1 and IL-8 promoters. p65 was absent at the promoters in unstimulated 1321N1 cells, but after 1-h stimulation with IL-1, p65 was detected at both promoters (Fig. 9a). This IL-1-induced promoter binding was not affected

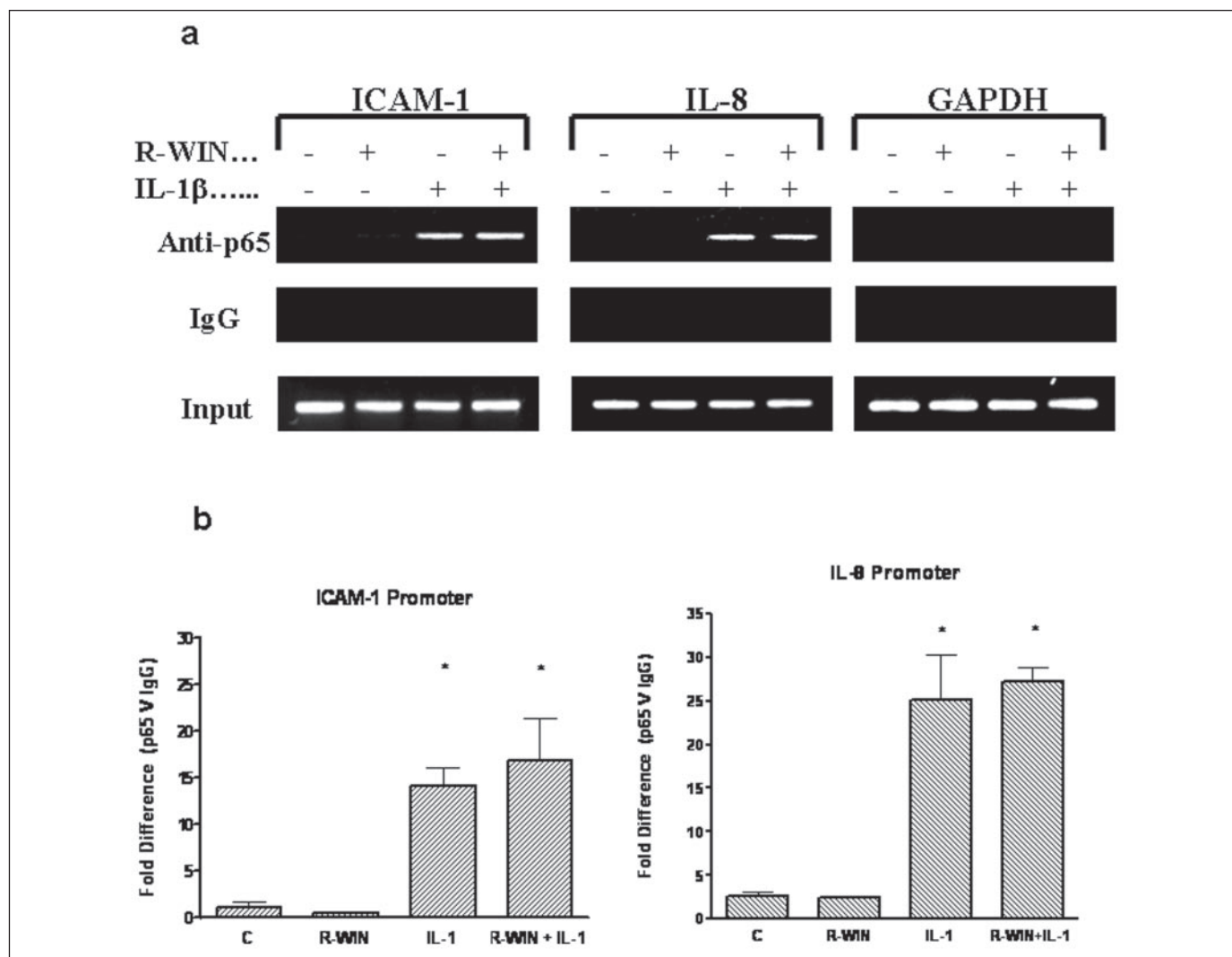


**FIGURE 9.** *R(+)*WIN 55,212-2 does not inhibit IL-1-induced binding of p65 to ICAM-1 or IL-8 promoters. 1321N1 astrocytoma were pre-treated with or without *R(+)*WIN 55,212-2 (20  $\mu$ M) for 1 h prior to stimulation for a further 1 h in the absence or presence of IL-1 $\beta$  (10 ng/ml). Chromatin immunoprecipitations were performed using anti-p65 or control IgG antibodies and DNA analyzed for ICAM-1, IL-8, and GAPDH promoters by PCR and gel electrophoresis (a) and quantitative real-time PCR (b). Data from real-time PCR are expressed as -fold differences between DNA enrichment in the anti-p65-ChIP sample relative to IgG-ChIP sample and are displayed as mean  $\pm$  S.E. from two independent experiments. These values were analyzed by one-way analysis of variance to determine statistical significance between treatments. \*, a value statistically significant ( $p < 0.05$ ) from the control value in untreated cells (c).

by pre-treatment with *R(+)*WIN 55,212-2. This was confirmed by quantitative real-time PCR analysis of the immunoprecipitated chromatin (Fig. 9b). One-way analysis of variance indicated that induction of p65 binding to both promoters by IL-1 was statistically significant in the absence or presence of *R(+)*WIN 55,212-2 pre-treatment, and there was no significant difference in the binding induced by IL-1 between these conditions. These findings suggest that *R(+)*WIN 55,212-2 does not interfere with the binding of NF $\kappa$ B to its promoters and must instead target the later stage of transactivation by NF $\kappa$ B.

We have previously shown that the only transactivating subunit of NF $\kappa$ B that is activated by IL-1 in 1321N1 cells is p65 (18). Because the activity of p65 is subject to regulation by phosphorylation at serine residues 276, 529, and 536, we sought to examine the potential regulation of phosphorylation of these sites by 276, 529, and 536 by *R(+)*WIN 55,212-2. Preliminary studies with phospho-specific antibodies failed to detect phosphorylation of residues 276 and 529 in response to IL-1 (data not shown) and thus these sites were not further explored. However using an antibody that specifically detects modified p65, which is phosphorylated at residue 536, it was possible to show that IL-1 caused

increased phosphorylation at this site (Fig. 10). However the pre-treatment of cells with *R(+)*WIN 55,212-2 failed to affect this phosphorylation suggesting that it inhibits the transactivation of NF $\kappa$ B by a novel mechanism.

## DISCUSSION

Cannabinoids exert many different effects in the brain, but much interest has recently focused on their neuroprotective value, and their promising potential as agents to treat neurological disorders such as multiple sclerosis. The aminoalkylindole *R(+)*WIN 55,212-2 is of special interest due its impressive therapeutic effects in ameliorating disease progression in animal models of multiple sclerosis (5, 6). Although the latter studies showed that *R(+)*WIN 55,212-2 inhibits leukocyte entry into the CNS and reduces the expression of pro-inflammatory cytokines the molecular mechanism underlying its effects was not addressed. In the present study we show that *R(+)*WIN 55,212-2 strongly inhibits the expression of the adhesion molecules VCAM-1 and ICAM-1 and the chemokine IL-8 in astrocytes. The reduced expression of adhesion molecules in astrocytes is likely to play a key role in medi-

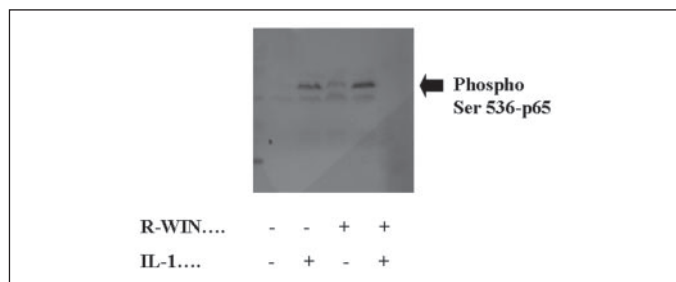


FIGURE 10. *R(+)*WIN 55,212-2 does not regulate IL-1-induced phosphorylation of p65 at serine residue 536. 1321N1 astrocytoma were pretreated for 1 h with *R(+)*WIN 55,212-2 (50  $\mu$ M) and stimulated for a further 30 min with IL-1 $\beta$  (10 ng/ml). Whole cell lysates were prepared and analyzed by Western immunoblotting for levels of p65 phosphorylated at residue 536 using an antibody that specifically reacts with this phosphorylated form of p65.

ating the therapeutic effects of *R(+)*WIN 55,212-2, because in acute multiple sclerosis lesions these adhesion molecules are strongly expressed in astrocytes (10), and strategies that interfere with their adhesive function inhibit leukocyte-astrocyte interactions (25) and reduce the severity of experimental multiple sclerosis (13). Furthermore the concentrations of *R(+)*WIN 55,212-2 that are required for manifesting inhibitory effects in the present study are comparable with the therapeutic doses used in the animal studies. In addition we found the chiral form *S(-)*WIN 55,212-2 to be inactive and this is consistent with its lack of effect in the animal models (5), thus further validating our experimental model.

Three independent approaches unambiguously dictate that the effects of *R(+)*WIN 55,212-2, with respect to inhibition of adhesion molecule expression in 1321N1 astrocytoma, are mediated by a mechanism independent of the CB1 and CB2 receptors. Firstly, selective antagonists for these receptors fail to influence the effects of *R(+)*WIN 55,212-2. Secondly, both receptors are coupled to a  $G_i$  protein and yet pertussis toxin, an inhibitor of this protein, has no effect on *R(+)*WIN 55,212-2. Lastly, the highly sensitive approach of RT-PCR failed to detect expression of either receptor in 1321N1 cells. Indeed the lack of expression of either receptor in the astrocytoma cells is consistent with previous reports showing their absence in primary astrocytes (26, 27). The non-polar nature of *R(+)*WIN 55,212-2 raises the possibility that its effects may be mediated via a nonspecific membrane-acting effect. However, this is highly unlikely on the basis of the stereoselectivity of the response to WIN 55,212-2. Indeed this work suggests the likely involvement of a novel receptor in mediating the inhibitory effects of *R(+)*WIN 55,212-2 in astrocytes.

*R(+)*WIN 55,212-2 exerted strong inhibitory effects on the IL-1-induced activation of the ICAM-1 and IL-8 promoters resulting in blockade of IL-1 induction of mRNAs encoding ICAM-1 and IL-8. This strongly suggests that *R(+)*WIN 55,212-2 inhibits the expression of such genes by targeting the transcription process or the upstream pathways that promote transcription. The NF $\kappa$ B pathway was chosen as a lead candidate target for *R(+)*WIN 55,212-2 due to its indispensable role in driving expression of pro-inflammatory proteins. *R(+)*WIN 55,212-2 caused strong inhibition of NF $\kappa$ B at the level of transactivation, because it inhibited the expression of a NF $\kappa$ B-regulated reporter gene but failed to affect the IL-1-induced degradation of I $\kappa$ B and the nuclear translocation and DNA binding activity of NF $\kappa$ B. This was confirmed in ChIP assays by the lack of effect of *R(+)*WIN 55,212-2 on the *in vivo* binding of the NF $\kappa$ B subunit p65 to the ICAM-1 and IL-8 promoters. In the ChIP studies, p65 was chosen as the target Rel subunit for a number of reasons. Firstly, it possesses transactivating ability (28). Secondly, the predominant form of NF $\kappa$ B activated by IL-1 in 1321N1

astrocytoma cells is the p65/p50 heterodimer (19). Furthermore studies have shown that the form of NF $\kappa$ B, which binds to the variant  $\kappa$ B sites in both the ICAM-1 and IL-8 promoters, is the p65 homodimer (29, 30). Although flanking elements in the promoters of these genes can influence the level of transcriptional activation, binding of p65 is an essential step in the IL-1-mediated induction of gene expression.

The mechanism by which *R(+)*WIN 55,212-2 targets NF $\kappa$ B remains to be resolved. The present studies suggest that *R(+)*WIN 55,212-2 does not regulate the phosphorylation of the p65 subunit at sites associated with regulation of transactivation. Indeed serine 536 was the only residue that we could show to be phosphorylated in response to IL-1, and this was not affected by *R(+)*WIN 55,212-2. This is hardly surprising, because IKK-2 has been proposed as the likely kinase responsible for phosphorylation of serine 536 and the lack of effect of *R(+)*WIN 55,212-2 on IL-1-induced degradation of I $\kappa$ B strongly suggests that IKK-2 is not a target for *R(+)*WIN 55,212-2. The targeting of transactivation of NF $\kappa$ B by *R(+)*WIN 55,212-2 differs significantly from the endocannabinoid anandamide that has been shown in T lymphocytes and adenocarcinoma cells to inhibit tumor necrosis factor activation of NF $\kappa$ B by targeting IKK-2 and blocking I $\kappa$ B degradation (31). This raises the interesting notion that *R(+)*WIN 55,212-2 may exert at least some of its effects by a mechanism that differs from the endocannabinoids.

The inhibitory effect of *R(+)*WIN 55,212-2 on NF $\kappa$ B transactivation is likely to be the key contributor to its ability to block IL-1 induction of adhesion molecule and chemokines expression in astrocytes and reduce leukocyte entry into the CNS. In addition the therapeutic effects of *R(+)*WIN 55,212-2 in a viral model of multiple sclerosis are associated with decreased transcription of the pro-inflammatory cytokines tumor necrosis factor, IL-1 and IL-6 that are strongly controlled by NF $\kappa$ B (5). The targeting of NF $\kappa$ B by *R(+)*WIN 55,212-2, as shown in the present study, is likely to be a key mechanism leading to the reduced expression of these pro-inflammatory cytokines.

The inhibition of the IL-1 signaling pathway by *R(+)*WIN 55,212-2 is also likely to be a key factor in manifesting the therapeutic effects of the latter in neuropathology. IL-1 has been shown to be a key regulator of neuro-inflammation and cell death in neurodegenerative conditions (32, 33). Interestingly, a recent report has shown that the anti-inflammatory and neuroprotective actions of cannabinoids in brain cells are mediated by the induction of the IL-1-receptor antagonist (34). The present study raises the intriguing concept that cannabinoids may target the IL-1 pathway not only by induction of an endogenous receptor antagonist but also by inhibition of the downstream signaling cascade.

In summary, the present study probes the molecular basis to the anti-inflammatory and therapeutic effects of cannabinoids in multiple sclerosis. It is proposed that the synthetic cannabinoid *R(+)*WIN 55,212-2 may produce anti-inflammatory effects by inhibiting NF $\kappa$ B, most likely at the level of transactivation. This increases our molecular appreciation of the potential use of cannabinoids in the treatment of neuropathological conditions.

REFERENCES

- Martino, G., Adorini, L., Rieckmann, P., Hillert, J., Kallmann, B., Comi, G., and Filippi, A. (2002) *Lancet Neurol.* **1**, 499–509
- Ungerleider, J. T., Andyrskiak, T., Fairbanks, L., Ellison, G. W., and Myers, L. W. (1987) *Adv. Alcohol Subst. Abuse* **7**, 39–50
- Consroe, P., Musty, R., Rein, J., Tillery, W., and Pertwee, R. (1997) *Eur. Neurol.* **38**, 44–48
- Meinck, H. M., Schonle, P. W., and Conrad, B. (1989) *J. Neurol.* **236**, 120–122
- Croxford, J. L., and Miller, S. D. (2003) *J. Clin. Invest.* **111**, 1231–1240
- Arevalo-Martin, A., Vela, J. M., Molina-Holgado, E., Borrell, J., and Guaza, C. (2003) *J. Neurosci.* **23**, 2511–2516
- Hafler, D. A., and Weiner, H. L. (1987) *Immunol. Rev.* **100**, 307–332
- Slipetz, D. M., O'Neill, G. P., Favreau, L., Dufresne, C., Gallant, M., Gareau, Y., Guay,

Downloaded from www.jbc.org by on August 19, 2009

## R(+)*WIN 55,212-2* Inhibits Interleukin-1 Signaling

- D., Labelle, M., and Metters, K. M. (1995) *Mol. Pharmacol.* **48**, 352–361
9. Ni, X., Geller, E. B., Eppihimer, M. J., Eisenstein, T. K., Adler, M. W., and Tuma, R. F. (2004) *Mult. Scler.* **10**, 158–164
10. Brosnan, C. F., Cannella, B., Battistini, L., and Raine, C. S. (1995) *Neurology* **45**, S16–S21
11. Cannella, B., and Raine, C. S. (1995) *Ann. Neurol.* **37**, 424–435
12. Hesselgesser, J., and Horuk, R. (1999) *J. Neurovirol.* **5**, 13–26
13. Yednock, T. A., Cannon, C., Fritz, L. C., Sanchez-Madrid, F., Steinman, L., and Karin, N. (1992) *Nature* **356**, 63–66
14. Kwon, D., Fuller, A. C., Palma, J. P., Choi, I. H., and Kim, B. S. (2004) *Glia* **45**, 287–296
15. Moynagh, P. N., Williams, D. C., and O'Neill, L. A. (1994) *J. Immunol.* **153**, 2681–2690
16. Rosenman, S. J., Shrikant, P., Dubb, L., Benveniste, E. N., and Ransohoff, R. M. (1995) *J. Immunol.* **154**, 1888–1899
17. Shrikant, P., Chung, I. Y., Ballesta, M. E., and Benveniste, E. N. (1994) *J Neuroimmunology* **51**, 209–220
18. Bourke, E., and Moynagh, P. N. (1999) *J. Immunol.* **163**, 2113–2119
19. Bourke, E., Kennedy, E. J., and Moynagh, P. N. (2000) *J. Biol. Chem.* **275**, 39996–40002
20. Schmitz, M. L., Bacher, S., and Kracht, M. (2001) *Trends Biochem. Sci.* **26**, 186–190
21. Saccani, S., Pantano, S., and Natoli, G. (2002) *Nat. Immunol.* **3**, 69–75
22. Chakrabarti, S. K., James, J. C., and Mirmira, R. G. (2002) *J. Biol. Chem.* **277**, 13286–13293
23. Herzberg, U., Eliav, E., Bennett, G. J., and Kopin, I. J. (1997) *Neurosci. Lett.* **221**, 157–160
24. Galiegue, S., Mary, S., Marchand, J., Dussosoy, D., Carriere, D., Carayon, P., Bouaboula, M., Shire, D., Le Fur, G., and Casellas, P. (1995) *Eur. J. Biochem.* **232**, 54–61
25. Hery, C., Sebire, G., Peudener, S., and Tardieu, M. (1995) *J. Neuroimmunol.* **57**, 101–109
26. Sagan, S., Venance, L., Torrens, Y., Cordier, J., Glowinski, J., and Giaume, C. (1999) *Eur. J. Neurosci.* **11**, 691–699
27. Walter, L., and Stella, N. (2003) *Glia* **44**, 85–90
28. Moore, P. A., Ruben, S. M., and Rosen, C. A. (1993) *Mol. Cell. Biol.* **13**, 1666–1674
29. Ledebur, H. C., and Parks, T. P. (1995) *J. Biol. Chem.* **270**, 933–943
30. Kunsch, C., Lang, R. K., Rosen, C. A., and Shannon, M. F. (1994) *J. Immunol.* **153**, 153–164
31. Sancho, R., Calzado, M. A., Di Marzo, V., Appendino, G., and Munoz, E. (2003) *Mol. Pharmacol.* **63**, 429–438
32. Rothwell, N. J., and Luheshi, G. N. (2000) *Trends Neurosci.* **23**, 618–625
33. Basu, A., Krady, J. K., and Levison, S. W. (2004) *J. Neurosci. Res.* **78**, 151–156
34. Molina-Holgado, F., Pinteaux, E., Moore, J. D., Molina-Holgado, E., Guaza, C., Gibson, R. M., and Rothwell, N. J. (2003) *J. Neurosci.* **23**, 6470–6474